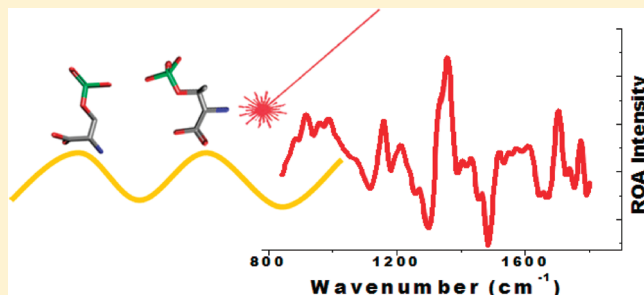


The Importance of Protonation in the Investigation of Protein Phosphorylation Using Raman Spectroscopy and Raman Optical Activity

Lorna Ashton,^{*,†} Christian Johannessen,[‡] and Royston Goodacre[†]

[†]School of Chemistry and [‡]Faculty of Life Sciences, Manchester Interdisciplinary Biocentre, University of Manchester, 131 Princess Street, Manchester, M1 7DN, U.K.

ABSTRACT: The effect of protonation on amino acid monomers and protein phosphorylation was studied by means of a combination of Raman scattering and Raman optical activity (ROA). In the past, identifying spectral variations in phosphorylated proteins arising from either the phosphate stretch or amide vibrational modes has proven to be challenging mainly due to the loss of amide and P=O band intensity in the presence of phosphate. By contrast, we have developed a novel strategy based on the careful monitoring of the sample pH and thereby modified the protonation state, such that these difficulties can be overcome and phosphate-derived vibrations are readily visualized with both Raman and ROA. Variations in pH-dependent spectral sets of phosphorylated amino acid monomers serine and threonine demonstrated that the protonation state could be determined by the intensity of the monobasic ($-\text{OPO}_3\text{H}^-$) phosphate stretch band occurring at $\sim 1080\text{ cm}^{-1}$ versus the dibasic ($-\text{OPO}_3^{2-}$) band measured at $\sim 980\text{ cm}^{-1}$ in both Raman and ROA. Furthermore, by adjustment of the pH of aqueous samples of the phosphoprotein α -casein and comparing this result with dephosphorylated α -casein, spectral variations in phosphate stretch bands and amide bands could be easily determined. Consequently, structural variations due to both protonation and dephosphorylation could be distinguished, demonstrating the potential of Raman and ROA for future investigations of phosphoprotein structure and interactions.



Following translation, many proteins undergo some type of chemical modification by the attachment to amino acids of additional biochemical functional groups including phosphates, carbohydrates, and lipids. An understanding of these post-translational modifications (PTMs) is extremely important as they result in changes to the physical and chemical properties of proteins, which alter their conformation, stability, and activity, and all ultimately help determine the function of the protein. Furthermore, the phosphorylation of protein by a kinase, or dephosphorylation by a phosphatase, can play an essential role in cellular processes. Reversible phosphorylation of seryl, threonyl, tyrosyl, or histidyl residues can induce ubiquitous mechanisms for controlling and regulating intracellular processes as well as inducing signal transduction networks.¹ Mass spectrometry (MS) is currently the main method employed in the investigation of protein phosphorylation, being utilized in the identification, measurement, and location of phosphorylation sites. However, MS is destructive, and obtaining quantitative information or monitoring structural mechanisms of the phosphorylation regulation processes by traditional structural biology techniques is often difficult and provides only limited insight.

The vibrational optical spectroscopic techniques of Raman scattering and Raman optical activity (ROA) have been shown to be potentially useful tools in monitoring structural mechanisms in proteins and in the identification of PTMs. Both techniques are extremely sensitive to perturbation induced conformational

changes, successfully facilitating the monitoring of protein unfolding^{2,3} as well as protein aggregation processes.^{4,5} It has also been well documented that Raman scattering techniques, including resonance Raman spectroscopy,⁶ surface-enhanced Raman scattering,⁷ and drop coating deposition Raman (DCDR)⁸ can be used in the detection of phosphate group signatures and phosphate-induced protein Raman spectral changes. In addition, ROA and Raman spectroscopy has been successfully applied to studies of glycoproteins identifying both the protein and carbohydrate components in the spectra,^{9,10} yet to date only limited success has been achieved with ROA investigations of phosphoproteins.^{4,11}

Jarvis et al.¹¹ demonstrated how the ratio of a phosphorylated and dephosphorylated protein, α -casein, could be determined by a combination of Raman spectroscopy and chemometric modeling. This work also investigated structural differences between the phosphorylated and dephosphorylated forms of α -casein using ROA, although these authors were able to determine protein structural differences, relating spectral variation directly to the phosphate-stretching bands proved difficult due to a lack of P=O vibrations observed in the phosphorylated protein spectrum. A further challenge of acquiring Raman and ROA spectra of phosphoproteins is a loss of intensity in the amide bands that can also occur making identification of both protein

Received: August 4, 2011

Accepted: September 15, 2011

Published: September 15, 2011

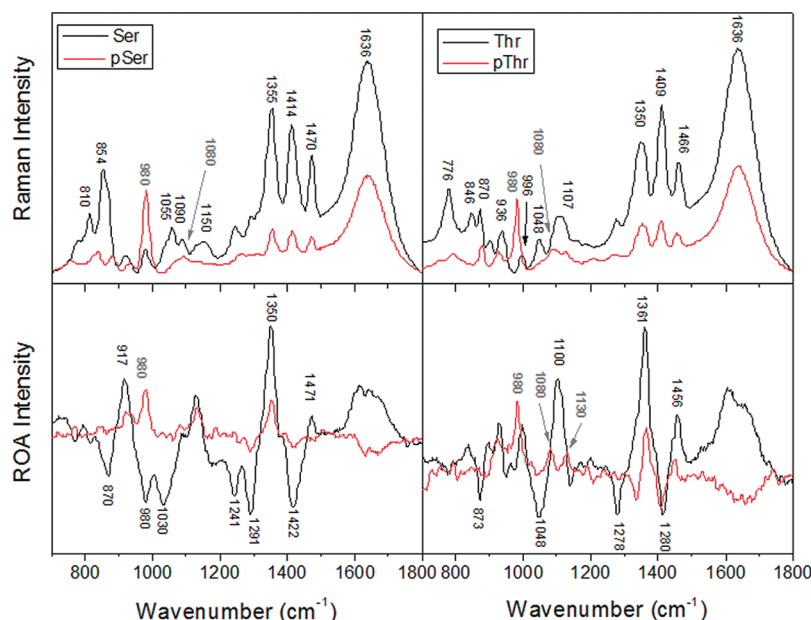


Figure 1. Raman and ROA spectra of L-serine (Ser) at \sim pH 6.1, L-threonine (Thr) at \sim pH 6.5, O-phospho-L-serine (pSer) at \sim pH 6.8, and O-phospho-L-threonine (pThr) at \sim pH 6.7 (accuracy ± 0.10 pH units).

and phosphate bands difficult.⁸ However, Xie and colleagues¹² demonstrated that changing sample pH dramatically alters the Raman spectra of phosphorylated peptides thus allowing “easier” identification of the phosphate and amino acid bands. They were able to use calibrated Raman band area ratio measurements, performed as a function of pH, to determine pK_a values.

In this study we have investigated the effect of modulating the pH of the environment, thus allowing regulation of the Raman and ROA spectra of the phosphorylated forms of the soluble amino acid monomers serine and threonine which resulted in the ready identification of phosphate stretch bands in ROA spectra of proteins. This has been extended and demonstrated with α -casein, which has allowed for the first time enhanced comparisons of the phosphorylated and dephosphorylated forms of this protein, and we believe this approach could have general utility for detailed investigations of other phosphoproteins.

EXPERIMENTAL SECTION

Samples and Analyses. Samples of L-serine (Ser), L-threonine (Thr), O-phospho-L-serine (pSer), O-phospho-L-threonine (pThr), α -casein, and dephosphorylated α -casein were purchased from Sigma (Dorset, U.K.) and used without any further purification. All solution samples were prepared by dissolving the dry material in distilled deionized H₂O. A small amount of charcoal was subsequently added to each sample to remove fluorescent impurities before it was minicentrifuged, and the supernatant was then filtered using a 0.22 μ m Durapore membrane filter. Spectra were collected immediately after preparation. All Raman and ROA measurements were performed using a ChiralRAMAN instrument (Biotools, Jupiter, FL)¹³ with the following experimental conditions: laser wavelength 532.5 nm, with laser power at the sample ~ 300 mW, the spectral resolution was ~ 7 cm⁻¹, and acquisition times were ~ 10 – 11 h. A digital pH meter (HANNAH Instruments, Woonsocket, RI) was used to measure

the final pH of each solution (accuracy ± 0.10 pH units). For the investigation of pH-dependent spectral variations, samples were prepared by adjusting the pH of the dry material dissolved in deionized H₂O with the addition of between ~ 5 – 70 μ L of 1 M NaOH solution. The final measured pH values for the seven separate pSer samples was \sim pH 2.0, 2.8, 4.1, 5.4, 6.8, 8.9, and 9.7 and \sim pH 1.8, 2.9, 5.2, 6.9, 9.2, 10.5, and 11.2 for the pThr samples. As well as samples prepared at the native pH (as described above), samples of α -casein and dephosphorylated α -casein were also prepared at \sim pH 13 with the addition of 1 M NaOH. Final concentrations for all samples were ~ 35 – 40 mg/mL.

Data Analysis. For further analysis of the pH-dependent spectral sets, we applied 2D correlation (2DCos) analysis. 2DCos is useful for monitoring dynamic fluctuations in spectra induced by some external perturbation on the system under analysis; in this case, the effect of pH on the amino acids or proteins results in different vibrational modes. 2DCos is based on a cross-correlation analysis of the perturbation-induced spectral set as a function of two independent wavenumber positions with the aim to enhance visualization of spectral fluctuations by spreading the data over a second dimension.¹⁴ All 2DCos calculations were carried out with the freely available 2D Shige software, using the perturbation-averaged spectrum as a reference spectrum in order to calculate the dynamic spectra.¹⁵ As has been extensively reported,^{14,16} for reliability and clarity 2DCos data need to be appropriately preprocessed. Before 2DCos calculations were applied, the data presented here were normalized to exposure time, baseline corrected, and smoothed using a fast Fourier transform (FFT) at 5 FFT points. All pretreatments were applied electronically with Origin 7.5 software (OriginLab, Northampton, MA). As also previously reported^{13,14} when the acquired spectral set is unevenly spaced, that is to say not measured using a fixed increment along the perturbation range as is the case in this study, 2DCos techniques cannot be directly applied.¹⁴ Two possible approaches have been suggested for further data pretreatment: Either to modify the original computational

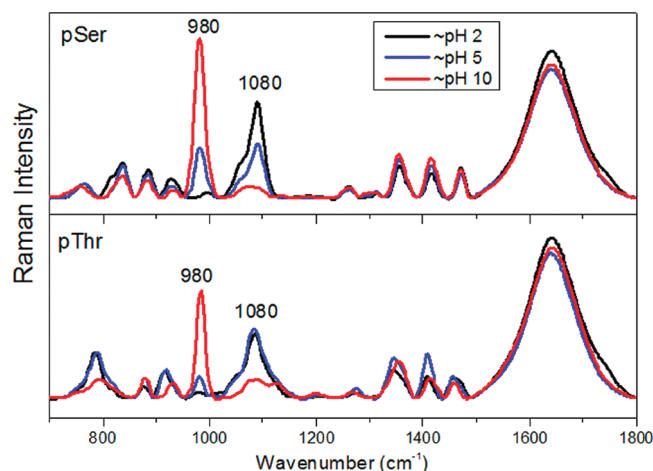


Figure 2. Raman spectra of *O*-phospho-L-serine (pSer) and *O*-phospho-L-threonine (pThr) at \sim pH 2, 5, and 10.

procedure with a numerical integration method or to convert the unevenly spaced data into evenly spaced data through interpolation or a simple curve fitting procedure.¹⁴ The latter interpolation procedure produces results that are based upon the underlying assumption that the dynamic system does not change significantly throughout the missing sections of data. As the data collected in this study varied in intensity in a consistent nature between samples, an interpolation procedure was performed with a Savitzky–Golay spline estimation to generate interpolated data consequently converting the unevenly spaced data to evenly spaced data before 2DCos calculations were applied.

RESULTS AND DISCUSSION

Amino Acid Monomers. Raman and ROA spectra of phosphorylated and nonphosphorylated serine and threonine monomers collected at \sim pH 6 are shown in Figure 1. A broad band at \sim 1636 cm^{-1} which can be assigned to the water H–O–H bending vibrations^{8,17} dominates the higher wavenumber ranges in all of these Raman spectra. Occasionally, the ROA spectra may also display weak broad features from the water above \sim 1600 cm^{-1} due to the instrumental setup not correctly canceling out all birefringent artifacts associated with the solvent Raman signals, and this results in the distortions observed in the ROA spectra in Figure 1. In agreement with previously reported Raman spectra,^{8,12} there is an overall loss of intensity for the majority of bands in the phosphorylated spectra compared to the nonphosphorylated amino acids. The ROA spectra in Figure 1 also show a loss of intensity in the $\text{C}\alpha$ -H and N–H bending region, equivalent to amide III in proteins (1230–1340 cm^{-1}) and in the skeletal stretching (870–1150 cm^{-1}) region.

Despite the suppression of Raman bands when phosphorylation is introduced, a clear phosphate stretching band can be observed at \sim 980 cm^{-1} in both Raman spectra of pSer and pThr. The intensity of this band measured at \sim 980 cm^{-1} is closely related to the pH of the samples. As previously discussed, Xie et al. demonstrated in their Raman study of amino acid monomer and peptide protonation¹² that changing the pH of solutions dramatically changes the Raman spectra. In pSer and pThr, a loss of intensity in the band at \sim 980 cm^{-1} and an increase in intensity in the band at \sim 1080 cm^{-1} can be observed as pH is lowered

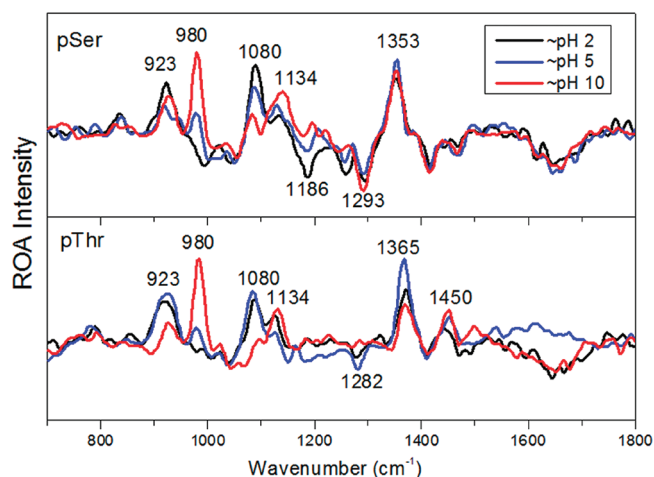


Figure 3. ROA spectra of *O*-phospho-L-serine (pSer) and *O*-phospho-L-threonine (pThr) at \sim pH 2, 5, and 10.

from \sim pH 10 to \sim pH 5 and disappears at \sim pH 2 (Figure 2). At pH 10, and under physiological pH conditions, it is expected that the phosphorylated monomers exist predominately in a dibasic form ($-\text{OPO}_3^{2-}$), where the negative charge is delocalized over the three oxygen atoms. As the pH becomes more acidic, the solution becomes a mixture of the dibasic and the monobasic ($-\text{OPO}_3\text{H}^-$) forms, and only once highly acidic conditions (pH < 2) are reached does stabilization of the fully protonated structure occur ($-\text{OPO}_3\text{H}_2$).^{1,12} Consequently, in the pSer and pThr Raman spectra shown in Figure 1, at \sim pH 6.5 and 6.7, respectively, a large band at \sim 980 cm^{-1} with a weaker band at \sim 1080 cm^{-1} can be observed due to the mixed protonation state of the samples.

Figure 3 displays a comparison of the pH-dependent ROA spectra of these two phosphorylated amino acids, although sets of seven spectra were collected over the pH range 2–10, and for the purpose of clarity, only three spectra measured at \sim pH 2, 5, and 10 are shown. Similar to the observations made in the Raman analysis, the ROA spectra of pSer and pThr exhibit a significant loss of intensity at \sim 980 cm^{-1} and a concomitant increase in intensity at \sim 1080 cm^{-1} when lowering the pH, indicating an equivalent sensitivity to the phosphate protonation state. Whereas the Raman spectra of the amino acid monomers only revealed two pH-dependent bands (Figure 2), more complex, and sample specific, variations can be observed between \sim pH 2–10 in the ROA spectra of pSer and pThr (Figure 3). These variations include minor intensity changes in the skeletal stretching region, specifically at \sim 923 cm^{-1} in the case of pThr and \sim 1186 cm^{-1} in the case of pSer, and even a possible nonlinear variation in the intensity of the \sim 1365 cm^{-1} $\text{C}\alpha$ -H bending mode of pThr. These observations indicate that ROA is more generally sensitive to the effects of the protonation state, which we have examined further through the use of 2D correlation analysis.

2D Correlation (2DCos) Analysis. We have previously applied 2DCos methods to investigate pH-induced conformational transitions in polypeptides and proteins and found that these significantly improve visualization and hence overall analysis and interpretation of these sets of spectral data.^{3,18} This approach is clearly highly appropriate for studying zwitterions such as amino acids and should aid in the interpretation of pH-dependent amino acid monomer spectra. 2DCos is a cross-correlation

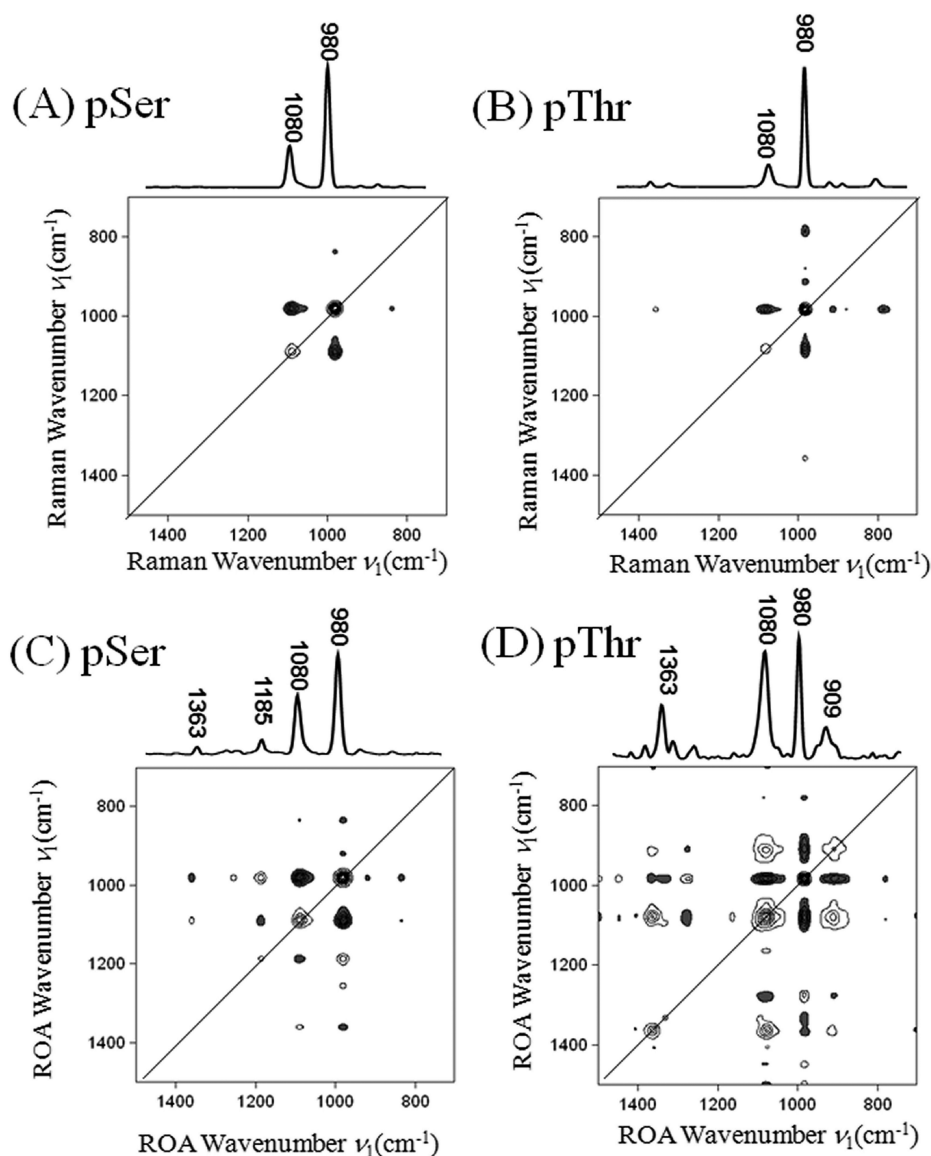


Figure 4. 2D synchronous plots with the autocorrelation plots of pH-dependent variations for the (A) Raman pSer, (B) Raman pThr, (C) ROA pSer, and (D) ROA pThr spectra calculated from spectral sets acquired at \sim pH 2–11. Gray shading indicates negative cross peaks, and no shading indicates positive cross peaks.

technique that is applied to a previously measured set of perturbation-induced spectra as a function of two independent wavenumber positions.^{14,19} This results in data matrices from which similarities and differences in behavior between bands occurring at two independent wavenumbers can be more readily identified. Several types of 2DCos matrices can be calculated including so-called synchronous and asynchronous spectra, which determine similarities and differences in behavior of spectral variations, respectively, and moving-window calculations which relate the data to the perturbation more directly in order to identify distinct phases in behavior.^{14,20,21} For the purposes of the present study, we have focused on the synchronous plots only as we are interested in comparing consistencies in behavior of phosphate related changes in the Raman and ROA data. These matrices may be displayed in a variety of ways including contour maps, stacked traces, or fishnet structures. Although the best overall view of the intensity profile of a correlation spectrum may be provided by stacked traces or pseudo-three-dimensional

figures, they may be difficult to interpret, and for the majority of 2DCos studies, contour plots are favored, as detailed peak shapes and positions may be more readily identified.

Figure 4 depicts the 2D synchronous contour plots with the autocorrelation plots of pH-dependent variations for the Raman and ROA spectra calculated from the interpolated spectral sets acquired over the range from pH 2 to 11. Synchronous contour maps consist of two types of contours positioned at general coordinates (ν_1, ν_2) autopeaks, which occur along the diagonal of the plot ($\nu_1 = \nu_2$) and identify bands of dynamic intensity change; and cross peaks, which indicate the existence of relative similarities in behavior between two independent bands positioned above or below the diagonal ($\nu_1 \neq \nu_2$). By definition, autopeaks are always positive, whereas cross peaks may be positive, represented in this paper by unshaded contours, or negative, denoted by contours shaded gray. The autocorrelation plots shown in Figure 4 are the diagonal values, or autopeaks, plotted as a function of intensity (arbitrary units) versus Raman

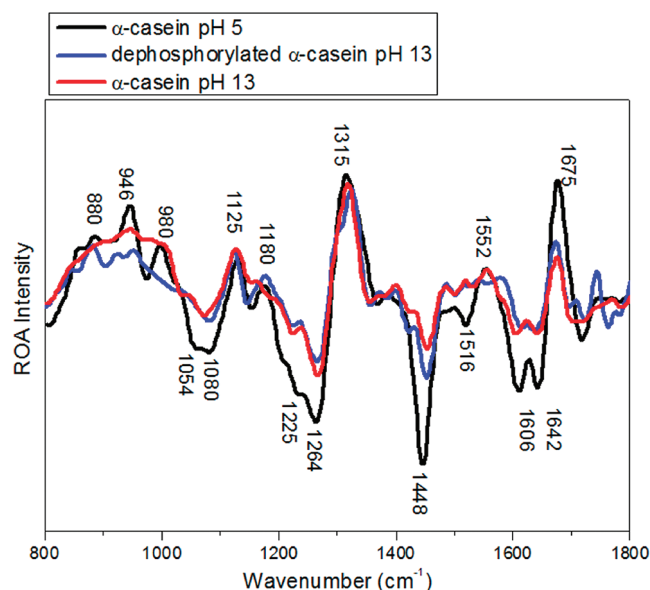


Figure 5. ROA spectra of phosphorylated α -casein at \sim pH 5 and 13 and dephosphorylated α -casein at pH 13.

or ROA wavenumber shift, and in this way the bands of the most dynamic spectral variance can be easily observed relative to each other. In both the Raman and ROA autocorrelations, the most intense peaks, and therefore bands of most dynamic spectral variance, can be observed at \sim 980 and 1080 cm^{-1} (dibasic band and monobasic phosphate stretch, respectively), further indicated by the large number of contours observed for cross peaks in the synchronous plots occurring at these wavenumber coordinates. These negative cross peaks occurring at (980,1080) correctly indicate that the two bands are changing in intensity in the opposite direction as pH decreases (loss of intensity in the band at \sim 980 cm^{-1} and an increase in intensity in the band at \sim 1080 cm^{-1}). A positive cross peak would indicate that both bands were changing in intensity in the same direction (either increasing or both decreasing in intensity).

When altering the pH of the samples, there is a possibility that the phosphate group could be cleaved from either pSer or pThr; however, the lack of observed cross peaks in the Raman 2D synchronous plots other than the already established phosphate stretch bands indicates that this has not occurred. If cleavage of the phosphate groups had occurred, one would expect to also observe the appearance of bands relating to newly formed C=C stretching modes and free HPO_4 .^{2–8} As the ROA data were collected simultaneously with the Raman data, it can also be assumed that none of the observed spectral variations are due to the cleavage of phosphate groups from the monomers. The autocorrelation plots for the ROA spectral sets (Figure 4) further reveal that more complex changes are occurring in the ROA spectra of both pSer and pThr as pH is altered, with spectral variations being observed at \sim 1185 and 1363 cm^{-1} in pSer and at \sim 909 and 1363 cm^{-1} in pThr. We believe that these variations also are monitoring the change from dibasic to monobasic forms of phosphate, registering minor conformational changes due to change in protonation state or even changes in solvent–solute interactions.

Phosphorylated Protein Measurements. In order to establish the sensitivity of ROA to the effects of the protonation state further, we compared the ROA spectra of α -casein at pH 5 and pH

13, along with dephosphorylated α -casein at pH 13 (Figure 5). Caseins have four major components recognized in cows' milk as α_{s1} , α_{s2} , and β - and κ -casein that are phosphorylated at 8, 9–11, 5, and 1 specific serine residues, respectively.^{11,22} α -caseins are relatively small proteins (\sim 200 amino acids/molecular weight \sim 25 kDa) and a mix of the two α_{s1} , α_{s2} components at a 4:1 ratio, therefore mostly the α_{s1} isoform. α -Casein proteins are involved in the transport of calcium and other metal ions to neonates but are also reported as having further roles including protection against heat coagulation, chaperone-like activity, binding to membrane receptors, and acting as signal transducers.²³ Previously, the general consensus regarding α -casein structure was that the proteins exhibited little, or no structural elements, but now it is accepted that although individually α -caseins have little or no tertiary structure, they have a polyproline type II (PPII) helical conformation giving rise to the rheomorphic properties of the proteins.⁴ One key advantage of ROA is its ability to record spectra of disordered peptides and unfolded proteins identifying less ordered protein features including the PPII helix which can not easily be observed in conventional Raman.²⁴

On initial examination, the majority of the α -casein ROA bands measured in Figure 5 can be observed to decrease in intensity as the pH is changed from pH 5 to pH 13 without any significant shifts in wavenumber. Caseins naturally assemble into complexes referred to as micelles^{22,25} and studies on the assembly of caseins have shown that the molecules can exhibit a progressive association to dimers, tetramers, hexamers, etc., which is highly dependent on pH, ionic strength, and the presence of calcium and it may be possible that the loss of intensity in the α -casein spectrum at pH 13 compared to pH 5 is due to a pH-induced clustering.²² However, as the main component of α -casein, the α_{s1} isoform, is sensitive to the presence of calcium, and as no calcium was added to the samples, it is unlikely that any clustering is occurring. Furthermore, during sample preparation, no visible change in turbidity was observed and if extensive clustering had occurred, the sample would have turned cloudy. Consequently, the loss of intensity is due to pH-induced changes in individual molecules and is most likely due to conformational changes in the single protein molecules.

Two bands that show spectral variation due to changes in phosphorylation and not pH can be observed at \sim 1315 and 1552 cm^{-1} . The intense positive band at \sim 1315 cm^{-1} can be assigned to the PPII structure.² A slight upward shift can be observed from \sim 1315–1324 cm^{-1} in the dephosphorylated spectra compared to the phosphorylated α -casein spectra at pH 5 and 13. This suggests a structural change as a result of the removal of the phosphate not directly caused by the change in pH. A similar change can be observed in the tryptophan assigned band at \sim 1552 cm^{-1} ²⁶ where a small positive band can be observed in phosphorylated α -casein at both pH 13 and 5 but not in the dephosphorylated spectrum. Jarvis et al.¹¹ previously reported the band at \sim 1552 cm^{-1} to be promoted upon dephosphorylation of α -casein due to this band monitoring conformational changes of the tryptophan residues.^{27,28} Subsequently, the changes observed at \sim 1552 cm^{-1} (Figure 5) may be monitoring a conformational change or change in orientation of tryptophan residues due to dephosphorylation and not the change in pH.

As previously discussed, in both Raman and ROA amino acid monomer spectra, the pH-dependent bands arising from the phosphate stretching vibrations are observed at \sim 980 and 1080 cm^{-1} , respectively, which is also observed in the ROA

spectra (Figure 5). At pH 13 and pH 5, the phosphate stretching band at $\sim 980\text{ cm}^{-1}$ is monitoring the dibasic form, while the monobasic assigned band at $\sim 1080\text{ cm}^{-1}$ is observed only at pH 5; neither band is observed in the dephosphorylated form. Consequently, with comparison of these three spectra, it is possible to determine for the first time the presence of phosphate stretching bands in α -casein ROA spectra.

CONCLUSIONS

Previous Raman and ROA investigations of phosphoproteins have been hampered by the suppression of amide bands combined with a lack of identifiable bands arising from phosphate stretching vibrations. However, we have demonstrated that with careful manipulation of the environmental pH, Raman and ROA spectroscopies do have the potential to investigate structural mechanisms resulting from phosphorylation of proteins. The bands occurring at ~ 980 and $\sim 1080\text{ cm}^{-1}$ in phosphorylated amino acids and phosphoproteins can be assigned to monobasic and dibasic forms of phosphate, respectively. In the pH-dependent Raman and ROA spectral sets of both pSer and pThr, a clear loss of intensity in the band at $\sim 980\text{ cm}^{-1}$ and an increase in intensity in the band at $\sim 1080\text{ cm}^{-1}$ can be observed as pH is lowered. If spectra of phosphoproteins are recorded at native pH, then the mix of these monobasic and dibasic populations can reduce the spectral intensity of either of the bands at ~ 980 and 1080 cm^{-1} . By adjustment of the pH of phosphoprotein solution samples, the relative populations will change accordingly, thus intensifying the appropriate phosphate stretching bands, allowing the protonation states of phosphoproteins to be assigned empirically. Furthermore, as demonstrated by the α -casein ROA spectra (Figure 5), comparison of spectra at different pH can also allow structural differences to be determined which can help with the identification of structural changes as a result of dephosphorylation. We believe this approach could have general utility for detailed investigations of other phosphoproteins, and this will be an area of future study.

AUTHOR INFORMATION

Corresponding Author

*E-mail: Lorna.Ashton@manchester.ac.uk. Fax: +44 (0) 1613064519.

ACKNOWLEDGMENT

We would like to thank the U.K. EPSRC and BBSRC and the industrial members of the Bioprocessing Research Industry Club (BRIC) for funding. We are also very grateful to Dr. Ewan Blanch for his support of this work.

REFERENCES

- (1) Wojciechowski, M.; Grycuk, T.; Antosiewicz, J. M.; Lesyng, B. *Biophys. J.* **2003**, *84*, 750–756.
- (2) Barron, L. D.; Blanch, E. W.; Hecht, L. *Adv. Protein Chem.* **2002**, *62*, 51–90.
- (3) Ashton, L.; Barron, L. D.; Hecht, L.; Hyde, J.; Blanch, E. W. *Analyst* **2007**, *132*, 468–479.
- (4) Syme, C. D.; Blanch, E. W.; Holt, C.; Jakes, R.; Goedert, M.; Hecht, L.; Barron, L. D. *Eur. J. Biochem.* **2002**, *269*, 148–156.
- (5) Xu, M.; Ermolenkov, V. V.; He, W.; Uversky, V. N.; Fredriksen, L.; Lednev, I. K. *Biopolymers* **2005**, *79*, 58–61.
- (6) Okishio, N.; Fukuda, R.; Nagai, M.; Nagai, Y.; Nagatomo, S.; Kitagawa, T. *J. Raman Spectrosc.* **1998**, *29*, 31–39.

- (7) Sundararajan, N.; Mao, D. Q.; Chan, S.; Koo, T. W.; Su, X.; Sun, L.; Zhang, J. W.; Sung, K. B.; Yamakawa, M.; Gafken, P. R.; Randolph, T.; McLerran, D.; Feng, Z. D.; Berlin, A. A.; Roth, M. B. *Anal. Chem.* **2006**, *78*, 3543–3550.
- (8) Zhang, D.; Ortiz, C.; Xie, Y.; Davisson, V. J.; Ben-Amotz, D. *Spectrochim. Acta, Part A* **2005**, *61*, 471–475.
- (9) Zhu, F.; Isaacs, N. W.; Hecht, L.; Barron, L. D. *Structure* **2005**, *13*, 1409–1419.
- (10) Brewster, V. L.; Ashton, L.; Goodacre, R. *Anal. Chem.* **2011**, *83*, 6074–6081.
- (11) Jarvis, R. M.; Blanch, E. W.; Golovanov, A. P.; Screen, J.; Goodacre, R. *Analyst* **2007**, *132*, 1053–1060.
- (12) Xie, Y.; Jiang, Y.; Ben-Amotz, D. *Anal. Biochem.* **2005**, *343*, 223–230.
- (13) Hug, W.; Hangartner, G. *J. Raman Spectrosc.* **1999**, *30*, 841–852.
- (14) Noda, I.; Ozaki, Y. *Two-Dimensional Correlation Spectroscopy: Applications in Vibrational and Optical Spectroscopy*; John Wiley and Sons Ltd.: Chichester, U.K., 2004.
- (15) <http://sci-tech.ksc.kwansei.ac.jp/~ozaki/e2D.htm>.
- (16) Ashton, L.; Czarnik-Matusiewicz, B.; Blanch, E. W. *J. Mol. Struct.* **2006**, *799*, 61–71.
- (17) Miura, T.; Thomas, G. J. In *Proteins: Structure, Function and Engineering*; Subcellular Biochemistry, Vol. 24; Biswas, B. B., Roy, S., Eds.; Plenum Press: New York, 1995; pp 55–99.
- (18) Ashton, L.; Blanch, E. W. *J. Mol. Struct.* **2010**, *974*, 132–138.
- (19) Noda, I. *Appl. Spectrosc.* **1993**, *47*, 1329–1336.
- (20) Morita, S.; Shinzawa, H.; Tsenkova, R.; Noda, I.; Ozaki, Y. *J. Mol. Struct.* **2006**, *799*, 111–120.
- (21) Ashton, L.; Blanch, E. W. *Appl. Spectrosc.* **2008**, *5*, 469–475.
- (22) Farrel, H. M.; Malin, E. L.; Brown, E. M.; Qi, P. X. *Curr. Opin. Colloid Interface Sci.* **2006**, *11*, 135–147.
- (23) Srinivas, S.; Kaul, P.; Prakash, V. *J. Agric. Food Chem.* **2007**, *55*, 9283–9288.
- (24) Zhu, F.; Kapitan, J.; Tranter, G. E.; Pudney, P. D. A.; Isaacs, N. W.; Hecht, L.; Barron, L. D. *Proteins Struct. Funct. Bioinf.* **2008**, *70*, 823–833.
- (25) Horne, D. S. *Curr. Opin. Colloid Interface Sci.* **2006**, *11*, 148–153.
- (26) Miura, T.; Takeuchi, H.; Harada, I. *J. Raman Spectrosc.* **1989**, *20*, 667–671.
- (27) Blanch, E. W.; Hecht, L.; Day, L. A.; Pederson, D. M.; Barron, L. D. *J. Am. Chem. Soc.* **2001**, *123*, 4863–4864.
- (28) Jacob, C. R.; Luber, S.; Reiher, M. *ChemPhysChem* **2008**, *9*, 2177–2180.